Smart sand by surface engineering: toward controllable oil/water separation

Jian Chang,[a,b] *Chisiang Ong,*[a,c] *Yusuf Shi,*[a] *Jiayin Yuan,**[b] *Zeyad Ahmed,**[d] *Peng Wang**[a,e]

[a]Water Desalination and Reuse Center, Division of Biological and Environmental Science and Engineering, King Abdullah University of Science and Technology, Thuwal 23955-6900, Saudi Arabia

[b]Department of Materials and Environmental Chemistry, Stockholm University, 10691 Stockholm, Sweden.

[c]School of Chemical and Biomedical Engineering, Nanyang Technological University, 62 Nanyang Drive, 637459, Singapore

[d]Water Treatment & Conservation Division, Environmental Protection Department, Saudi Aramco, Dhahran 31311, Saudi Arabia

[e]Department of Civil and Environmental Engineering, The Hong Kong Polytechnic University, Hong Kong, China

Corresponding author e-mail: jiayin.yuan@mmk.su.se, zeyad.ahmed@aramco.com,

peng.wang@kaust.edu.sa

ABSTRACT:

Sand, as an abundant resource from the nature, is a promising candidate for oil/water separation. Herein, raw sand was designed with a switchable surface wettability to enable recyclability and versatility in practical oil/water separation. The "smart" sand was fabricated by grafting pH-responsive poly(4-vinylpyridine) (P4VP) and oleophilic/hydrophobic octadecyltrimethoxysilane (OTS) onto its surface. The derocated sand can be used as the oil sorbent for controllable oil sorption and desorption in response to different pHs, as well as a filter to selectively separate either oil or water on demand. This novel design offers an intelligent, low cost, large-scale, and highly efficient route to potentially settle the issues of industrial oily wastewater and oil spills.

1. INTRODUCTION

With the increasing amount of industrial oily wastewater and frequent accidents of crude oil spill, a cost-effective and efficient oil/water separation technology based on "smart" materials is highly desired.[1-2] In the past decade, the remarkable progress in advanced interfaces with super-wettability towards water or oil has made a sound contribution to the development of the next generation oil/water separation systems, particularly in adsorption- and filtration-based separation, by using modified sponge, mesh, textile, membrane, *etc.*[1, 3-6] Although the oil/water separation efficiency of the materials ever reported is promising, their real-life application at scale remains restricted due to the complicated surface modification processes, high materials cost, and low recyclability during practical oil/water separation.

The raw sand, a rich resource across the entire planet, can be abundantly obtained from the deserts, river and seashore. Owing to its natural superhydrophilic and underwater superoleophobic properties, the raw sand carries the merits of excellent water absorption and ultralow oil adhesion capability that are beneficial for oil/water separation.[7-12] In addition to the low materials and possible operating cost, the benefits of using sand as the oil/water separation materials also include their tunable operating scales that can be easily controlled by adjusting the amount of sand used.[9, 13] Furthermore, considering the recyclability and versatility requirement for oil-water separation processes in the practical application, it is highly desirable to have the separation materials with controllable surface wettability, which can be modulated by external stimuli.[1, 4, 6] By using responsive materials with switchable wettability, the absorbed oil can be easily recovered, and the smart materials can be reused in a sustainable and cost-effective manner for the oily wastewater treatment or oil spill cleanup.[2] Among them, the pH-responsive ones are attractive due to their fast wettability switch triggered by the changes of pH.[14-24] The developed materials possess switchable oil wettability under different pHs, which can be used for controllable oil/water separation processes. Nevertheless, smart sand has never been developed for the oil/water separation.

Herein, the smart sand with pH-responsive oil wettability was for the first time fabricated for oil/water separation by grafting poly(4-vinylpyridine) (P4VP) and octadecyltrimethoxysilane (OTS) onto the surface of silica particles pre-modified raw sand. The as-prepared smart sand displayed highly switchable superoleophilicity and superoleophobicity under water in response to different pHs, which allows for its easy regeneration in aqueous solutions at room temperature. It could effectively absorb oil that can be rapidly released upon acid treatment. It

also shows a promising oil/water separation with a high water flux for immiscible oil/water mixture driven by gravity, as well as excellent recyclability.

2. EXPERIMETAL SECTION

2.1. Materials

Raw sand was directly obtained from the desert in Thuwal, Saudi Arabia and was cleaned with ethanol and deionized water sequentially in an ultrasonic cleaner before use. Cetyltrimethyl ammonium bromide (CTAB), tetraethoxysilane (TEOS), (3-bromopropyl)trimethoxysilane (BPS), poly(4-vinylpyridine) (P4VP), hexadecane, ethanol, hexane, petroleum ether, oil red O and anhydrous toluene were all purchased from Sigma-Aldrich. Kerosene was purchased from Ricca chemical company. Hydrochloric acid (HCl) and ammonium hydroxide was ordered from Fisher Chemical. Octadecyl-trimethoxy-silane (OTS) and methylene blue were purchased from Acros Organics. Crude oil (density: 0.9 g/mL, API gravity: 32.6, viscosity: 31 mPa·s) was received from Ali I. Al-Naimi Petroleum Engineering Research Center, KAUST. All chemicals were used as received. Deionized water purified by Milli-Q system was used in all experiments.

2.2. Fabrication of SiO_2 modified sand

To obtain the SiO_2 modified sand, the surface of raw sand was first modified to be positively charged. In doing so, 100 mL of 50 mg/mL CTAB aqueous solution was added to 25 g of sand in 200 mL ethanol solution, and then the mixture was stirred for 1 h. Afterwards, the pH value of the mixture solution was adjusted to 12 by using ammonium hydroxide. 20 mL TEOS was then added drop-wise to the above mixture followed by continuous and vigorous stirring for 12 h for

silica coating. Finally, the SiO_2 modified sand was rinsed with deionized water followed by drying in an oven at 60 °C.

2.3. Fabrication of smart sand

25g of SiO_2-modified sand was added into a 200 ml of toluene solution containing 2g of BPS and OTS to functionalize the sand surface with bromoalkyl groups and alkyl groups *via* silanization. The ratio of BPS and OTS was set as 0:10, 1:9, 3:7, 5:5, 7:3, 9:1, 0:10, respectively. After continuous and vigorous stirring for 12 h at room temperature, the silanized sand was rinsed with toluene and ethanol to remove the unreactive siloxane followed by drying in the oven at 60 °C. The dried silanized sand was then added into 1 wt% ethanol solution of P4VP under stirring for 1 h. Finally, the smart sand was obtained by heating under vacuum at 150 °C for 12 h to enable quaternization between the bromoalkyl groups of BPS and the pyridine groups of P4VP. The unreactive polymers were removed by washing with copious amounts of ethanol.

2.4. Characterization

Scanning electron microscopy (SEM) images were taken with a Zeiss Merlin scanning electron microscope. Contact angles (CAs) were measured on a commercial contact angle system (OCA 35 of DataPhysics, Filderstadt, Germany) at ambient temperature. The X-ray photoelectron spectroscopy (XPS) was carried out on a Kratos Axis Ultra instrument under ultrahigh vacuum conditions in the range of $\sim 10^{-9}$ mbar by using a monochromatic Al Kα X-ray source ($h\upsilon = 1486.6$ eV) operated at 150 W. The weight of sand was measured by digital balance (Mettler Toledo).

2.5. Controllable sorption and desorption of oil

Hexadecane dyed with oil red O was placed onto the surface of water in a glass bottle. Then a proper amount of the smart sand was added into the glass bottle. Hexadecane was adsorbed directly by the smart sand, and the saturated oily sand then sank to the bottom of the glass bottle driven by gravity. To release the hexadecane from the hexadecane-loaded smart sand, a certain amount of acidic water with pHs range from 1 to 3 was placed into the glass bottle to change the oil wettability of the smart sand.

2.6. Controllable separation of oil and water mixtures

To perform the separation of oil and water mixtures, a layer of smart sand with different thickness from 1 to 4 cm was fixed between two glass tubes with a diameter of 16 mm, serving as a separator. A piece of non-woven textile was placed below the sand to prevent the sand from being lost. With the non-acidic pretreated smart sand placed between two glass tubes, a mixture of hexadecane dyed with oil red O and water of pH 6.5 dyed with methylene blue in a ratio of 3:1 was poured into the upper glass tube, and the separation was achieved driven by gravity. The hexadecane successfully passed through the sand layer, whereas the water remained in the upper glass tube. For the acidic water-treated smart sand, the smart sand was first pre-wetted with acidic water with a pH of 2.0 before the separation process. Then a mixture of hexadecane dyed with oil red O and pH 6.5 water dyed with methylene blue in a ratio of 1:3 was poured into the same filtration system. Water selectively passed through the sand layer, whereas hexadecane remained in the upper glass tube.

3. RESULTS AND DISCUSSION

3.1. The fabrication of the smart sand

Compared with the recently used organic and inorganic substrate materials, the advantages of desert sand include its mechanical and chemical stability, environmental friendliness, and its abundance in nature.[7-9] Any raw sand with the lateral size > 0.6 mm could be sieved out by the stainless steel mesh before its surface modification. Figure S1 shows the raw sand particles have an average particle size of 0.27±0.08 mm in lateral dimension. Generally, to achieve super-wettability, the substrate material should possess sufficient surface roughness in order to amplify its intrinsic wetting behavior.[25-31] Herein, SiO_2 particles were modified onto the raw sand (Sand@SiO_2) *via* the hydrolysis of TEOS in an alkaline environment.[7, 32] Figure 1a and 1b show that the raw sand possessed a very smooth surface, while the surface of the Sand@SiO_2 became rougher due to the presence of silica nanoparticle aggregates on its surface (Figure 1c-d).

To fabricate the smart sand, the as-prepared Sand@SiO_2 was first modified with BPS and OTS under a defined mixing ratio. The surface grafted OTS provides low surface energy chains to give hydrophobicity to the smart sand under non-acidic condition. The modification of BPS is to functionalize the surface of the sand with bromoalkyl groups *via* silanization, which serves as a binder for subsequent grafting of P4VP on its surface (Figure 1e). Then the P4VP polymer was grafted onto the surface of previously silanized Sand@SiO_2 through the quaternization reaction between the bromoalkyl groups of BPS and the pyridyl groups of P4VP by heating under vacuum at 150 °C for 12 h. The grafted P4VP endows the sand surface with a pH-responsive wettability.[18-20, 24]

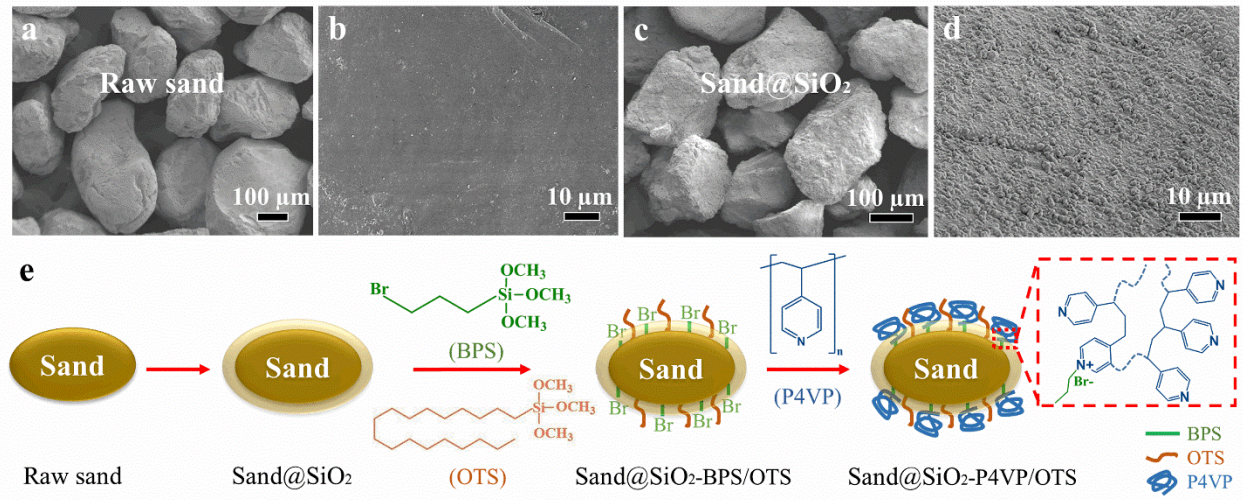

Figure 1. SEM images of (a-b) raw sand and (c-d) the SiO_2-modified sand (Sand@SiO_2). Scale bar: 100 μm and 10 μm. (e) Schematic diagram of preparation of SiO_2 modified sand (Sand@SiO_2), BPS and OTS modified Sand@SiO_2 (Sand@SiO_2-BPS/OTS) and smart sand (Sand@SiO_2-P4VP/OTS).

To confirm the successful chemical modification of the sand, its surface was analyzed by XPS. The raw sand shows significant Si and O peaks around 100 eV (Si 2p), 150 eV (Si 2s), and 530 eV (O 1s), with possible minor C 1s contaminants at around 285 eV (Figure 2a). This result agrees with the fact that the raw sand is mainly composed of silica.[7-8] Additionally, the characteristic peaks of some metal elements (Mg, Ca, Al, and Fe) are also observed in the spectrum of raw sand due to the co-existence of few metal species in the sand. In comparison with the raw sand, the characteristic peaks of metal species are not obvious on Sand@SiO_2, indicating the SiO_2 coating layer fully covering the entire surface of the sand (Figure 2b). The appearance of Br 3d peak of Sand@SiO_2-BPS/OTS suggests that the BPS was successfully grafted onto the sand surface *via* silanization (Figure 2c). As for the smart sand final product, a unique N signal peak that appears at around 400 eV (N 1s) can be assigned to the nitrogen of the pyridine groups from P4VP polymer, indicating the successful grafting of P4VP onto the surface

of the smart sand (Figure 2d-e). Furthermore, as shown in Figure 2f, the high resolution C 1s core-level spectra further confirm the modification of P4VP on the modified sand surfaces due to the presence of the polymer backbone C-C peak at 284.4 eV, aromatic C-C at 285.0 eV, and aromatic C-N at 285.5 eV. Meanwhile, the EDS mapping images of the smart sand surface also clearly show that the C and N elements associated with P4VP was uniformly present on the sand surface (Figure S2).

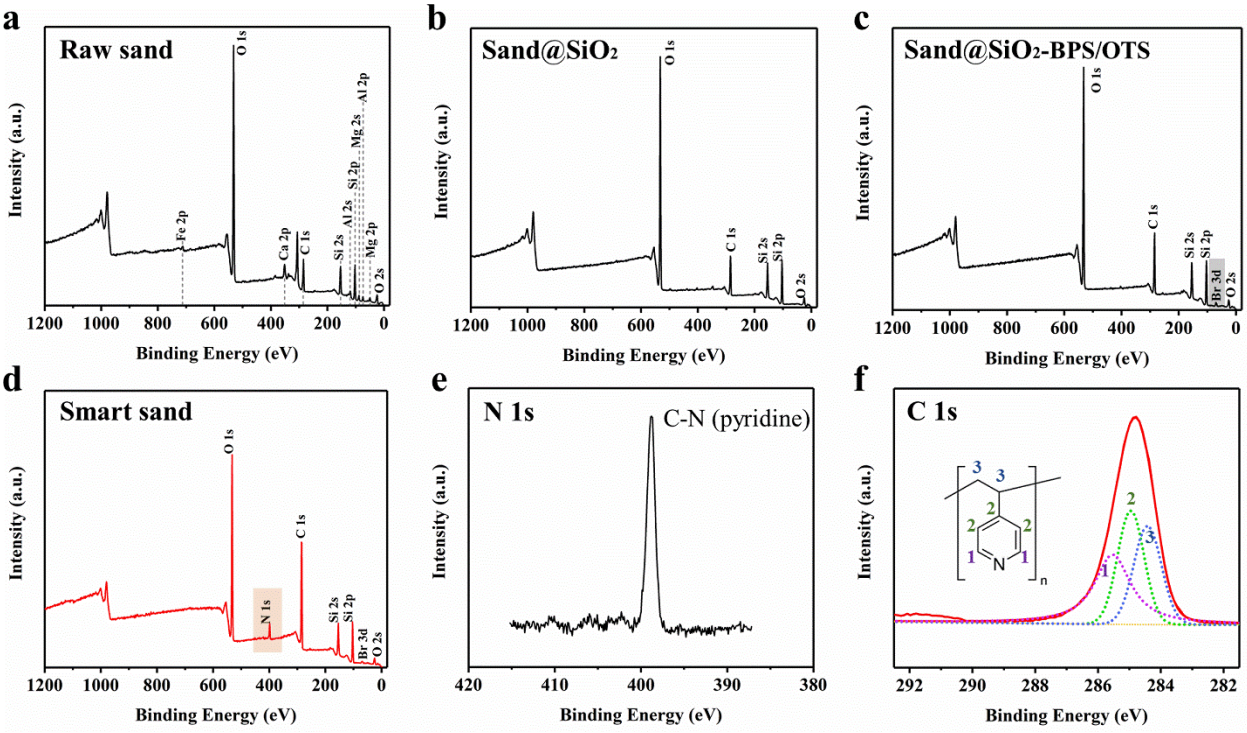

Figure 2. XPS spectra of (a) the raw sand, (b) Sand@SiO_2, (c) Sand@SiO_2-BPS/OTS and (d) the smart sand. The high resolution spectra of (e) N 1s and (f) C 1s of the smart sand.

3.2 Wettability of the smart sand.

The original raw sand surface is covered with a large number of hydroxyl groups, metal species and silica dioxide with a high surface free energy, thus endowing the surface with intrinsic

hydrophilicity and oleophilicity in air (Figure S3).[7-8, 10] After the successful modification of both P4VP and OTS, the surface wettability of the smart sand surface possesses switchable wettability between superhydrophilicity and hydrophobicity in response to the change of the pH of aqueous solution from 1.0 to 6.5 (Figure S4).

As shown in Figure 3a, the as-prepared smart sand exhibits hydrophobicity in the air with a water contact angle (WCA) of 136°, which can be attributed to the presence of OTS on the surface, as well as the deprotonation state of P4VP. Furthermore, it shows a mirror-like sand surface underneath water because the air trapped around the hydrophobic sand prevents the water permeating into the interstice among sands (Figure S5a). In addition to hydrophobicity, the oleophilicity of OTS also endows the sand surface with high affinity to oil. The oil droplet can be immediately adsorbed into the smart sand surface within 0.05s, exhibiting its superoleophilicity in the air (Figure 3b). The smart sand is also able to capture oil underwater (ESI Movie 1), indicating its underwater superoleophilicity.

However, when an acidic water droplet of pH 2.0 was placed on the surface of the smart sand in the air, the water droplet was quickly adsorbed into the surface within 4 s (Figure 3c, ESI Movie 2), indicating the pH-responsive switchable wettability of the smart sand surface. Furthermore, the oil wettability of this smart sand can be completely reversed when it is immersed in acidic water. The smart sand exhibits an underwater oleophobicity with an underwater oil contact angle (OCA) of 138° in the acidic water of pH 2.0 (Figure 3d, Figure S5b), which confirms its switchable oil wettability in low-pH solution. In addition, such oil droplet can roll off easily from the sand surface, showing a sliding angle of 7° (ESI Movie 3) and indicating the low oil adhesion of the smart sand surface in the acidic water.

The switchable wettability of the smart sand is significantly affected by the ratio of BPS and OTS, which determines the ratio between P4VP and OTS in the final product. As shown in Figure 3e, the WCA of the smart sand at pH 6.5 increased from 62º to 150º by increasing the ratio of OTS over BPS owing to the increasing amount of hydrophobic OTS on the surface. Meanwhile, the surface wettability of the smart sand could be switched to superhydrophilicity (WCA: 0º) at pH of 2.0, which can be well-maintained until the ratio of BPS and OTS was adjusted to 3:7. Further increase in the amount of OTS significantly increases the WCA of the smart sand and the surface becomes hydrophobic. This is because lowering the amount of BPS might cause the significant decrease of grafted P4VP onto the silanized Sand@SiO_2 *via* quaternization, leading to the loss of superhydrophilicity of smart sand at pH of 2.0.

Based on the results mentioned above, the switchable wettability of the smart sand is primarily dependent on the amount of the surface P4VP and OTS. At pH of 6.5, the P4VP is deprotonated and exhibits a collapsed conformation. Correspondingly, more hydrophobic OTS chains could dominantly expose itself to air, which turns the surface into hydrophobic and retains its high affinity to oil. By contrast, at pH of 2.0, the pyridyl groups of P4VP are protonated considering its pKa of approximately 3.5~4.5.[16, 33] The protonated P4VP chains exhibit an extended conformation due to the electrostatic repulsion among the like-charges (Figure 3e, Inset). Thus, they tend to stretch and expose to the sand surface, resulting in the formation of hydrophilic layer onto the sand surface. In addition, this hydrophilic layer could effectively block the access of oil by the OTS, which endows the smart sand with superior oil-repellency ability at low pH.

Besides, the acidic-water treated sand can easily recover its hydrophobicity and oleophilicity after being rinsed with pure water and then dried in the air. This reversible cycle can be repeated

many times without any significant decline observed in its switchable wettability (Figure S6), indicating that the formation of P4VP on the sand is very stable.

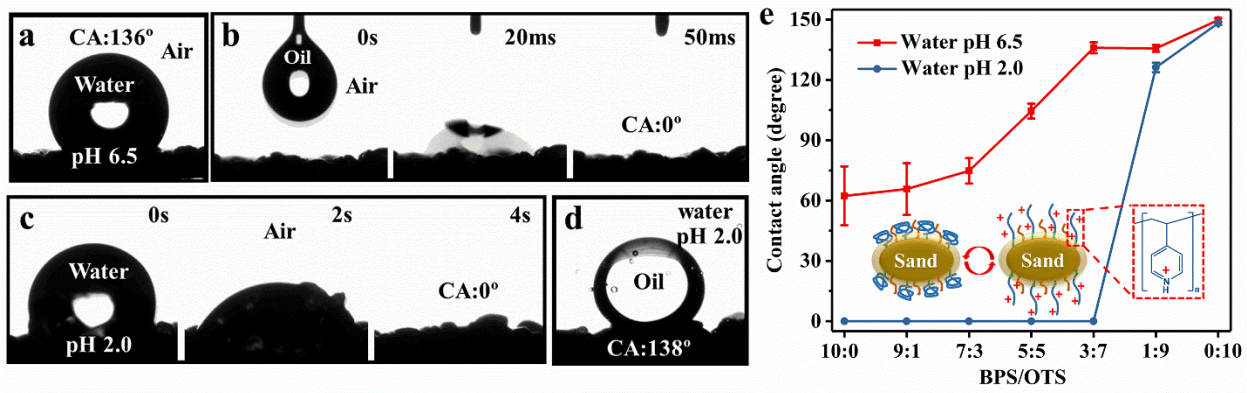

Figure 3. (a) The image for a water droplet (pH~ 6.5) applied on the smart sand surface in air. (b) Still images from the OCA measurements of an oil droplet (hexadecane) applied on the smart sand surface in the air. (c) Still images from the WCA measurements for a water droplet (pH~ 2.0) applied on the smart sand surface. The acidic water droplet was quickly absorbed into the sand surface within 4s. (d) The image of an oil droplet applied on the surface of the smart sand in water at pH of 2.0. (e) The wettability of the smart sand for water droplets at pH of 2.0 (blue line) and 6.5 (red line) by tuning the ratio of BPS and OTS. Inset: schematic diagram of the pH-responsive mechanism of P4VP.

3.3 Controllable oil absorption and desorption

Based on the above-mentioned switchable wettability performance, the smart sand could then be used for oil sorption and desorption in aqueous media at different pHs. As illustrated in Figure 4a, an oil layer was placed onto the water surface at pH 6.5. Once the smart sand was in contact with the oil layer spreading on the water surface, it instantaneously absorbed the oil from the surface and sank to the bottom of the glass bottles driven by its own gravity due to its superoleophilic properties. Moreover, the absorbed oil droplets could be spontaneously released

from the sand by immersing the oil-loaded sand into acidic water at pH 1.0 (Figure 4a, ESI Movie 4), indicating its switchable surface wettability at low pH condition.

To further understand the effect of different pHs on the oil desorption capacity of the smart sand, the saturated oily sand was treated by acidic water at different pHs (Figure 4b). The oil desorption capacity is calculated by the weight ratio of the released oil and the absorbed oil. The absorbed oil (1.0 g) was quickly released from the smart sand within 2 min with almost no residual oil in the sand (≥99%) under water at pH 1.0. However, with the same amount of absorbed oil, it might take nearly 12 min with around 91% of oil desorption from the smart sand under water of pH 2.0. And there was no oil released from the smart sand observed at pH ≥ 3.0. Additionally, such sorption and desorption cycle was successfully realized with various oils, *i.e.*, hexadecane, petroleum ether, kerosene and hexane and these results can be clearly seen in Figure S7. Besides that, the smart sand can realize controllable absorption and desorption of the highly viscous crude oil (ESI Movie 5).

This is attributed to the protonated pyridyl groups of P4VP at pH < 3, generating a surface of superhydrophilicity and underwater oleophobicity and thus leading to the weak affinity between smart sand surface and oil. Accordingly, the rate of oil releasing from sand can be adjusted, where lowering pH can make the oil releasing faster and more efficient owing to the generation of more protonated pyridyl groups in a shorter time.[18] Nevertheless, at pH higher than 3, the deprotonated P4VP remains its collapsed conformation and the OTS still dominantly exposes to the outer layer, leading to the hydrophobicity and oleophilicity of the smart sand. Therefore, no oil is released. This also agrees well with the contact angle measurements that the WCA of the smart sand at pH 3 is around 114° (Figure S4).

Furthermore, the smart sand maintains its pH responsiveness even after 6 cycles of oil sorption and desorption process (Figure 4c). Unlike conventional recovery of oil/water separation materials by using mechanical squeezing or rinsing by organic solvent,[34] this smart sand can be repeatedly used in aqueous solutions at room temperature without generating secondary waste organic solvent or destroying the material structure. Besides, the smart sand can be molded into any shape on demand, due to random accumulation of the sand particles. This unique advantage is distinctly different from conventional oil/water separation materials and would be able to decrease the overall material amount and the related operating costs.

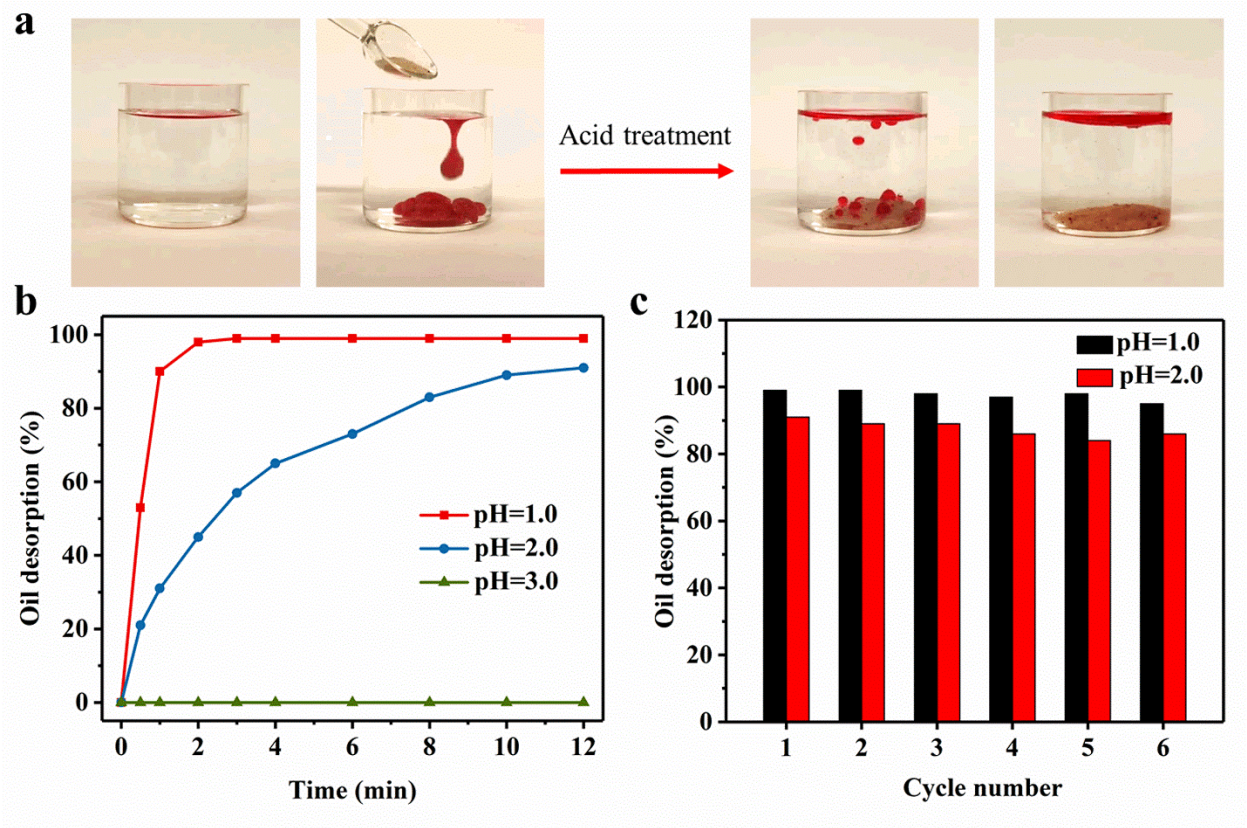

Figure 4. (a) Snapshots showing the sorption of the oil (hexadecane stained with oil red O dye) by the smart sand in water at pH 6.5, as well as the release of the captured oil after acid treatment. (b) The oil desorption capacity of saturated oily smart sand *versus* time in water at

different pH values. (c) The oil desorption capacity of saturated oily smart sand in different cycling tests in water at pH of 1 and 2.

3.4 Controllable oil/water separation.

The smart sand can act as a separating membrane for controllable oil/water separation owing to its switchable superoleophilicity and superoleophobicity. As shown in Figure 5a, a layer of smart sand was fixed between two glass tubes with a piece of non-woven textile placing below the sand to prevent the sand from being lost. Then, a mixture of oil and water at pH 6.5 was poured into the upper glass tube. Based on the superoleophilicity and high hydrophobicity of the smart sand, the oil quickly passed through the sand layer, but the water was retained on top of the sand layer in the upper glass tube (ESI Movie 6). Nevertheless, once the sand layer was pre-wetted by acidic water at pH 2.0, the opposite separation phenomenon could be realized (Figure 5b, ESI Movie 7). That is, the water quickly passed through the sand layer while the oil was completely retained on top of the sand layer in the glass tube due to the formation of a hydrated layer caused by the protonation of P4VP. Similar separation process is also available for a mixture of water and highly viscous crude oil (ESI Movie 8)

During the controllable separation processes, the water and oil fluxes of the sand layer with different thickness of the sand layer were calculated by measuring the time for an oil/water mixture of a certain volume to permeate through. As shown in Figure 5c, both oil and water fluxes decreased with the increase in the thickness of the sand layer (from 1 to 4 cm) due to a longer effective penetration distance. When the thickness of the sand layer is 1 cm, the oil and water flux can reach up to 2906 and 9556 L m^{-2} h^{-1}, respectively. Furthermore, the difference in

the water and oil fluxes (J) and their respective flux behaviors with the thickness of sand layer could be explained by Hagen-Poiseuille equation:

$$J = \frac{\varepsilon \pi r_p 2\Delta p}{8\mu L}$$

Where, ε is the surface porosity, r_p is the pore radius, Δp is the pressure drop, μ is the viscosity of penetrating solution, and L is the effective filtrate distance.[35] As described on the formula above, the filtrate flux (J) is inversely proportional to the effective filtrate distance (L). In addition, the flux is also inversely proportional to the viscosity of penetrating solution (μ). Therefore, the water flux (viscosity: 1.002 mPa s at 20 ºC for water) is higher than that of oil (viscosity: 3.474 mPa s at 20 ºC for hexadecane).

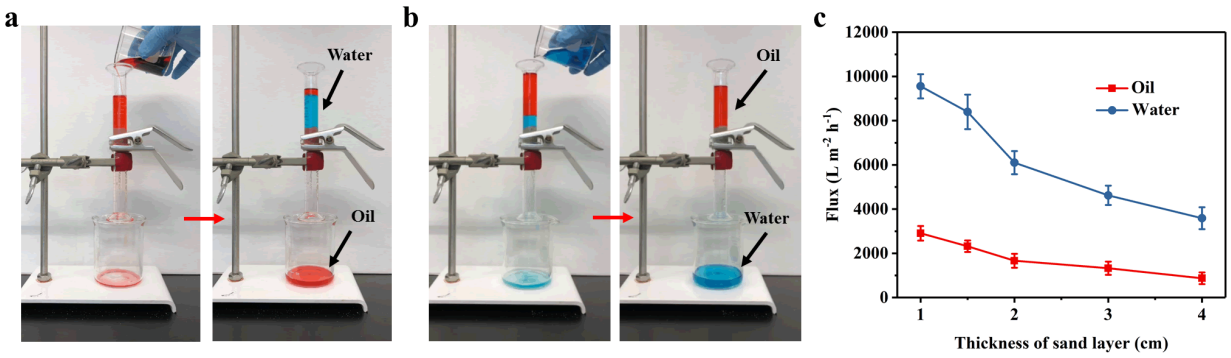

Figure 5. (a) The smart sand was fixed between two glass tubes as the separation membrane. A mixture of oil (hexadecane dyed with oil red O) and water (dyed with methylene blue) was poured into the upper glass tube. The oil selectively passed through the sand layer, while the water remained in the upper glass tube. (b) When the smart sand was first wetted by acidic water (pH 2.0) before the oil/water separation process, water selectively passed through the sand layer, while oil remained in the upper glass tube. (c) The influence of the thickness of the smart sand layer on the fluxes of water (blue line) and oil (red line).

4. CONCLUSIONS

In conclusion, we prepared the smart sand by grafting pH-responsive P4VP and oleophilic/hydrophobic OTS onto the sand surface and demonstrated its switchable wettability for controllable oil absorption/desorption. In terms of the filtration-based separation, either oil or water could selectively pass through or remain on top of the sand on demand, which is suitable for oil removal from wastewater with an oil density either higher or lower than water. This intelligent, low cost, large-scale, and highly efficient route of oil/water separation will offer a new perspective on solving the problems of practical oily industrial wastewater and oil spills.

ASSOCIATED CONTENT

Supporting Information

EDS mapping, still images, contact angles, photograph, and oil desorption capacity

Movies S1-S8 (ZIP)

CONFLICTS OF INTEREST

There are no conflicts to declare.

ACKNOWLEDGMENT

We would like to thank King Abdullah University of Science and Technology (KAUST) and Saudi Aramco for generous funding to support this project (RGC/3/3577-01-01).

REFERENCES

1. Wang, B.; Liang, W.; Guo, Z.; Liu, W., Biomimetic super-lyophobic and super-lyophilic materials applied for oil/water separation: a new strategy beyond nature. *Chem. Soc. Rev.* **2015,** *44*, 336-361.
2. Chang, J.; Zhang, L.; Wang, P., Intelligent environmental nanomaterials. *Environ. Sci. Nano* **2018,** *5*, 811-836.

3. Ma, Q.; Cheng, H.; Fane, A. G.; Wang, R.; Zhang, H., Recent development of advanced materials with special wettability for selective oil/water separation. *Small* **2016,** *12*, 2186-2202.
4. Xue, Z.; Cao, Y.; Liu, N.; Feng, L.; Jiang, L., Special wettable materials for oil/water separation. *J. Mater. Chem. A* **2014,** *2*, 2445-2460.
5. Lee, C. H.; Tiwari, B.; Zhang, D.; Yap, Y. K., Water purification: oil-water separation by nanotechnology and environmental concerns. *Environ. Sci. Nano* **2017,** *4*, 514-525.
6. Chu, Z.; Feng, Y.; Seeger, S., Oil/water separation with selective superantiwetting/superwetting surface materials. *Angew. Chem. Int. Ed.* **2015,** *54*, 2328-2338.
7. Chen, L.; Si, Y.; Guo, Z.; Liu, W., Superhydrophobic sand: a hope for desert water storage and transportation projects. *J. Mater. Chem. A* **2017,** *5*, 6416-6423.
8. Yong, J.; Chen, F.; Yang, Q.; Bian, H.; Du, G.; Shan, C.; Huo, J.; Fang, Y.; Hou, X., Oil-water separation: a gift from the desert. *Adv. Mater. Interfaces* **2016,** *3*, 1500650.
9. Men, X.; Ge, B.; Li, P.; Zhu, X.; Shi, X.; Zhang, Z., Facile fabrication of superhydrophobic sand: Potential advantages for practical application in oil-water separation. *J. Taiwan Inst. Chem. Engrs.* **2016,** *60*, 651-655.
10. Li, J.; Xu, C.; Guo, C.; Tian, H.; Zha, F.; Guo, L., Underoil superhydrophilic desert sand layer for efficient gravity-directed water-in-oil emulsions separation with high flux. *J. Mater. Chem. A* **2018,** *6*, 223-230.
11. Mosayebi, E.; Azizian, S.; Cha, B. J.; Woo, T. G.; Kim, Y. D., Fabrication of highly hydrophobic sand@soot with core-shell structure and large-scale production possibility for oil/water separation. *J. Phys. Chem. Solids* **2021,** *150*, 109815.
12. Mosayebi, E.; Azizian, S.; Noei, N., Preparation of robust superhydrophobic sand by chemical vapor deposition of polydimethylsiloxane for oil/water separation. *Macromol. Mater. Eng.* **2020,** *305*, 2000425.
13. Atta, A. M.; Abdullah, M.; Al-Lohedan, H. A.; Mohamed, N. H., Novel superhydrophobic sand and polyurethane sponge coated with silica/modified asphaltene nanoparticles for rapid oil spill cleanup. *Nanomaterials* **2019,** *9*, 187.
14. Tantavichet, N.; Pritzker, M. D.; Burns, C. M., Proton uptake by poly (2-vinylpyridine) coatings. *J. Appl. Polym. Sci.* **2001,** *81*, 1493-1497.
15. Gohy, J.-F.; Lohmeijer, B. G.; Varshney, S. K.; Décamps, B.; Leroy, E.; Boileau, S.; Schubert, U. S., Stimuli-responsive aqueous micelles from an ABC metallo-supramolecular triblock copolymer. *Macromolecules* **2002,** *35*, 9748-9755.
16. Franck-Lacaze, L.; Sistat, P.; Huguet, P., Determination of the pKa of poly (4-vinylpyridine)-based weak anion exchange membranes for the investigation of the side proton leakage. *J. Membr. Sci.* **2009,** *326*, 650-658.
17. Pinkrah, V.; Snowden, M.; Mitchell, J.; Seidel, J.; Chowdhry, B.; Fern, G., Physicochemical properties of poly (N-isopropylacrylamide-co-4-vinylpyridine) cationic polyelectrolyte colloidal microgels. *Langmuir* **2003,** *19*, 585-590.
18. Lei, Z.; Zhang, G.; Deng, Y.; Wang, C., Surface modification of melamine sponges for pH-responsive oil absorption and desorption. *Appl. Surf. Sci.* **2017,** *416*, 798-804.
19. Yang, J.; Loh, X. J.; Tan, B. H.; Li, Z., pH-responsive poly (dimethylsiloxane) copolymer decorated magnetic nanoparticles for remotely controlled oil-in-water nanoemulsion separation. *Macromol. Rapid Commun.* **2018,** *40*, 1800013.
20. Maaz, M.; Elzein, T.; Dragoe, D.; Bejjani, A.; Jarroux, N.; Poulard, C.; Aubry-Barroca, N.; Nsouli, B.; Roger, P., Poly (4-vinylpyridine)-modified silica for efficient oil/water separation. *J. Mater. Sci.* **2019,** *54*, 1184-1196.

21. Zhang, L.; Zhang, Z.; Wang, P., Smart surfaces with switchable superoleophilicity and superoleophobicity in aqueous media: toward controllable oil/water separation. *NPG Asia Mater.* **2012,** *4*, e8.
22. Li, J.-J.; Zhou, Y.-N.; Jiang, Z.-D.; Luo, Z.-H., Electrospun fibrous mat with pH-switchable superwettability that can separate layered oil/water mixtures. *Langmuir* **2016,** *32*, 13358-13366.
23. Zhu, H.; Chen, D.; Li, N.; Xu, Q.; Li, H.; He, J.; Lu, J., Graphene foam with switchable oil wettability for oil and organic solvents recovery. *Adv. Funct. Mater.* **2015,** *25*, 597-605.
24. Li, J.-J.; Zhou, Y.-N.; Luo, Z.-H., Smart fiber membrane for pH-induced oil/water separation. *ACS Appl. Mater. Interfaces* **2015,** *7*, 19643-19650.
25. Tuteja, A.; Choi, W.; Ma, M.; Mabry, J. M.; Mazzella, S. A.; Rutledge, G. C.; McKinley, G. H.; Cohen, R. E., Designing superoleophobic surfaces. *Science* **2007,** *318*, 1618-1622.
26. Quéré, D., Wetting and roughness. *Annu. Rev. Mater. Res.* **2008,** *38*, 71-99.
27. Gao, L.; McCarthy, T. J.; Zhang, X., Wetting and superhydrophobicity. *Langmuir* **2009,** *25*, 14100-14104.
28. Liu, K.; Yao, X.; Jiang, L., Recent developments in bio-inspired special wettability. *Chem. Soc. Rev.* **2010,** *39*, 3240-3255.
29. Li, Y.; Li, L.; Sun, J., Bioinspired self-healing superhydrophobic coatings. *Angew. Chem. Int. Ed.* **2010,** *49*, 6129-6133.
30. Li, X.-M.; Reinhoudt, D.; Crego-Calama, M., What do we need for a superhydrophobic surface? A review on the recent progress in the preparation of superhydrophobic surfaces. *Chem. Soc. Rev.* **2007,** *36*, 1350-1368.
31. Wang, B.; Zhang, Y.; Shi, L.; Li, J.; Guo, Z., Advances in the theory of superhydrophobic surfaces. *J. Mater. Chem.* **2012,** *22*, 20112-20127.
32. Bai, X.; Xue, C.-H.; Jia, S.-T., Surfaces with sustainable superhydrophobicity upon mechanical abrasion. *ACS Appl. Mater. Interfaces* **2016,** *8*, 28171-28179.
33. Satoh, M.; Yoda, E.; Hayashi, T.; Komiyama, J., Potentiometric titration of poly (vinylpyridines) and hydrophobic interaction in the counterion binding. *Macromolecules* **1989,** *22*, 1808-1812.
34. Chang, J.; Shi, Y.; Wu, M.; Li, R.; Shi, L.; Jin, Y.; Qing, W.; Tang, C.; Wang, P., Solar-assisted fast cleanup of heavy oil spills using a photothermal sponge. *J. Mater. Chem. A* **2018,** *6*, 9192-9199.
35. Peng, X.; Jin, J.; Nakamura, Y.; Ohno, T.; Ichinose, I., Ultrafast permeation of water through protein-based membranes. *Nat. Nanotechnol.* **2009,** *4*, 353-357.

Abstract Graphics